Multi-user MIMO with Jamming Suppression for Spectrum-Efficient Tactical Communications

Qingqing Cheng*, Zhipeng Lin*, J. Andrew Zhang*, Diep Nguyen*,
Xiaojing Huang*, Asanka Kekirigoda† and Kin-Ping Hui†
* Global Big Data Technologies Centre, University of Technology Sydney, Sydney, Australia
† Defence Science and Technology (DST), Edinburgh, Australia
Emails: {Qingqing.Cheng; Zhipeng.Lin}@student.uts.edu.au; {Andrew.Zhang; Diep.Nguyen;
Xiaojing.Huang}@uts.edu.au; {Asanka.Kekirigoda; Kinping.Hui}@dst.defence.gov.au

Abstract—Being spectrum-efficient and robust to adversarial interference caused by jammers are critical to tactical wireless systems. Leveraging multiple-input multiple-output (MIMO) techniques, this paper investigates the realization of spectrum-efficient multi-user MIMO communications in the presence of high-power jammers. Unlike most existing work that only exploits the MIMO degree of freedom to nullify the jamming signal, we also aim to improve the spectral efficiency of the system with the MIMO spatial multiplexing capability. To that end, we first design a combiner at the receiver spanning the null space of the jamming channels, which can completely remove the jamming signals and optimize the communication reception. We further propose two methods for the design of precoders at the transmitter to mitigate multi-user interference. Simulation results are presented to verify the effectiveness of the proposed scheme in radio-frequency contested environments.

Index Terms—Anti-jamming, Tactical communication, MIMO, Beamforming, SDMA

I. INTRODUCTION

Tactical wireless communication systems operate in complex terrain and radio frequency (RF) contested environments. Compared to single antenna systems, multiple-input-multiple-output (MIMO) techniques can largely increase system capacity and mitigate interference in the spatial domain, hence, they have been proposed for tactical communications [1]–[4].

Numerous MIMO-based anti-jamming methods have been investigated to suppress jamming in tactical RF environments [5]–[9]. In [5], an adaptive transmit-receive beamforming scheme was proposed for MIMO system, using subspace projection to determine the transmitter and receiver beamforming. An anti-jamming method in [7] was developed based on null-steering to cope with malicious jamming in Long Term Evolution (LTE) military communications. In [8], a tactical MIMO communication system was developed to mitigate interference from multiple jammers. In most of these anti-jamming works, however, multi-user MIMO (MU-MIMO) or spatial division multiplexing access (SDMA), which provides independent spatial streams between multiple users, are not realized. That is, existing anti-jamming algorithms in MIMO systems are not able to simultaneously mitigate the multi-user interference and the interference caused by multiple jammers. More recently, joint SDMA and jamming suppression was investigated for a multi-user wireless network in the presence

of an adversarial jammer [10]. Interference alignment techniques are adopted for jamming suppression and multipoint-to-multipoint communications. However, the solution requires complicated signal processing and iterative communication between different users.

In this work, we investigate the realization of simultaneous jamming suppression and MU-MIMO in a tactical communications system, with efficient MU-MIMO precoding and combining techniques. Specifically, we propose a scheme with novel algorithms that can support MU-MIMO while simultaneously suppressing jamming signals. Our scheme only requires one feedback of equivalent channels, and hence largely reduces the network overhead. We assume the presence of high power jammers, so suppressing jamming signals is regarded as a priority. In principle, our scheme supports the suppression of multiple jammers, where each jammer can have multiple antennas. We first design a beamforming matrix for each user that falls in the null space of jamming channels. Consequently, jamming can be completely suppressed/nullified when the channel estimation is ideal. We further develop the joint transmitter precoder and receiver combiner, only requiring the feedback of the equivalent channel after the combiner is firstly designed. Our scheme is shown to be very efficient in suppressing jamming signals, while supporting MU-MIMO communications with low complexity and feedback overhead.

The remainder of this paper is organized as follows. Section II describes the system model and problem formulation. In Section III, the proposed anti-jamming algorithm is presented. Section IV shows numerical simulation results, and conclusions are provided in Section V.

Notations: We use $(.)^T$, $(.)^*$, $(.)^H$, and $(.)^{-1}$ for transpose, conjugate, conjugate (Hermitian) transpose, and inverse operation, respectively.

II. PROBLEM FORMULATION

For the convenience of presentation, we present our scheme by referring to an access network with multiple users and a base station (BS), and we focus on the downlink, i.e., the BS sends multiple spatial streams to multiple users. The scheme can also be applied to other networks such as military ad-hoc networks where one node uses SDMA to communicate to multiple other users in the presence of high-power jammers.
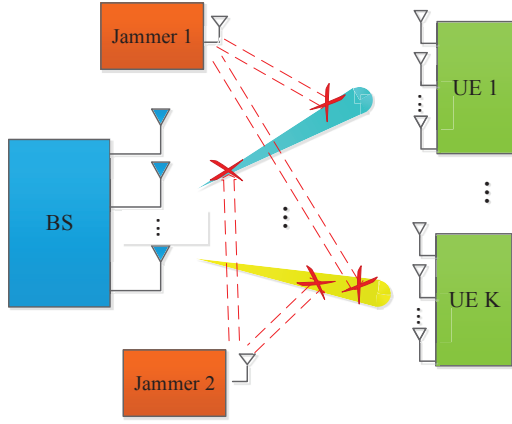
Fig. 1. Block diagram of MU-MIMO with two jammers

Consider such an MU-MIMO downlink system in a contested environment, with N_T transmit antennas at the BS and N_k receive antennas at the kth user equipment (UE), as illustrated in Fig. 1. The BS communicates to K UEs using MU-MIMO. Note that in a typical tactical network, the BS, which can often be converted from a normal node, does not necessarily have many more antennas than UEs. There are J jammers that intend to jam communications between BS and UEs. Each jammer equips N_J antennas and continuously transmit high-power random signals for jamming purpose. The number of independent data streams for UE k is S_k, where $S_k \leq N_k$, and $S = \sum_{k=1}^{K} S_k$ is the total number of independent streams. Note that at the minimum, we only require $N_T \geq S$ for MU-MIMO, and $N_k > J$ for effective jamming suppression and signal reception. More antennas at BS and UE can certainly lead to better performance. We do not require channel reciprocity here, and our scheme can be applied to both time division duplex (TDD) and frequency division duplex systems. The channel in each communication link is modelled as a slow (quasi-static) Rician fading channel.

Let $\mathbf{P}_k$ be the precoding matrix applied at the BS for UE k, with size of $N_T \times S_k$. The received signals at the kth UE is given by

$$\mathbf{y}_k = \mathbf{H}_k \mathbf{P}_k \mathbf{x}_k + \mathbf{H}_k \sum_{i \neq k}^{K} \mathbf{P}_i \mathbf{x}_i + \sum_{j=1}^{J} \mathbf{Z}_{k,j} \mathbf{f}_j + \mathbf{n}, \quad (1)$$

where $\mathbf{H}_k \in \mathbb{C}^{N_k \times N_T}$ denotes the channel matrix between the BS and UE k; $\mathbf{Z}_{k,j} \in \mathbb{C}^{N_k \times N_J}$ is the channel matrix between jammer j and UE k; $\mathbf{x}$ and $\mathbf{f}$ stand for the signals transmitted from the BS and jammers, respectively; and $\mathbf{n}$ is the background noise which is modelled as an additive white Gaussian noise (AWGN) with independent and identically distributed (i.i.d.) entries of zero mean and variance σ^2. We assume that $\mathbf{H}_k$ and $\mathbf{Z}_k = [\mathbf{Z}_{k,1}, \cdots, \mathbf{Z}_{k,J}]$ are known to UE k. Due to its non-cooperative nature, the jamming channels can generally be estimated by using blind channel estimation schemes or using signal projection techniques [11]. If line-of-sight (LOS) path is dominating then this can be performed through jamming localization techniques [12].

For a transmitter-receiver pair, $\mathbf{H}_k$ is given by

$$\mathbf{H}_k = \sum_{l=1}^{L} \upsilon_{k,l} \mathbf{a}_k(\theta_{a,l}) \mathbf{a}_k(\theta_{d,l})^T, \quad (2)$$

where $\upsilon_{k,l}$ is UE k's amplitude of complex value accounting for both signal attenuation and initial phase difference; $\mathbf{a}_k(\theta_{a,l})$ and $\mathbf{a}_k(\theta_{d,l})$ are the steering vectors of the transmitter and receiving arrays, respectively, and L is the number of total propagation paths. We consider a uniform circular array (UCA) in this paper, and $\mathbf{a}_k(\theta_{a,l}) = [e^{j\pi \cos(\theta_{a,l})}, ..., e^{j\pi \cos(\theta_{a,l} - 2\pi(N_k - 1)/N_k)}]^T$, with $\theta_{a,l}$ denoting the angle-of-arrival (AoA) from the l-th path; $\mathbf{a}_k(\theta_{d,l}) = [e^{j\pi \cos(\theta_{d,l})}, ..., e^{j\pi \cos(\theta_{d,l} - 2\pi(N_T - 1)/N_T)}]^T$, with $\theta_{d,l}$ denoting the angle-of-departure (AoD) from the l-th path.

Similarly, for the jammer channel $\mathbf{Z}_{k,j}$, it can be expressed as

$$\mathbf{Z}_{k,j} = \sum_{l=1}^{L} \upsilon_{j,l} \mathbf{a}_j(\phi_{a,l}) \mathbf{a}_j(\phi_{d,l})^T, \quad (3)$$

where $\upsilon_{j,l}$ stands for jammer j's amplitude of complex value accounting for both signal attenuation and initial phase difference; $\mathbf{a}_j(\phi_{a,l}) = [e^{j\pi \cos(\phi_{a,l})}, ..., e^{j\pi \cos(\phi_{a,l} - 2\pi(N_k - 1)/N_k)}]^T$, with $\phi_{a,l}$ denoting AoA value from the l-th path; and $\mathbf{a}_j(\phi_{d,l}) = [e^{j\pi \cos(\phi_{d,l})}, ..., e^{j\pi \cos(\phi_{d,l} - 2\pi(N_J - 1)/N_J)}]^T$, with $\phi_{d,l}$ denoting AoD from the l-th path.

III. PROPOSED SCHEME FOR JAMMING SUPPRESSION AND SDMA

In this section, we first provide an overview for the proposed scheme, then describe detailed designs for each component.

A. Overview of Proposed Scheme

Our proposed scheme consists of three steps: jamming suppression at UE receivers, combiner design at UE receivers, and precoder design at BS. The first step is done independently by each UE, and the last two steps can be designed jointly between BS and UEs. Specifically, the overall processing for UE k can be mathematically represented by the following equation

$$\mathbf{q}_k = \mathbf{W}_{bk}^H \times$$
$$\underbrace{\mathbf{W}_{ak}^H \left(\mathbf{H}_k \mathbf{P}_k \mathbf{x}_k + \mathbf{H}_k \sum_{i \neq k}^{K} \mathbf{P}_i \mathbf{x}_i + \sum_{j=1}^{J} \mathbf{Z}_{k,j} \mathbf{f}_j + \mathbf{n} \right)}_{\mathbf{r_k}},$$
$$(4)$$

where $\mathbf{W}_{ak} \in \mathbb{C}^{N_k \times S_k}$ is used to nullify the jamming signals and construct an optimized equivalent channel for communication, and $\mathbf{W}_{bk} \in \mathbb{C}^{S_k \times S_k}$ is used to equalize the equivalent channels $\mathbf{W}_{ak}^H \mathbf{H}_k \mathbf{P}_k$.

Since jamming signals have high power, jamming can be more detrimental to the receiver compared to multi-user signals. Hence the key idea in the first step is to nullify the jamming signals by exploiting the N_k degrees-of-freedom offered by multiple antennas. Specifically, we project the

received signal (with jamming) onto a space that is orthogonal to the jamming signal, so that the jamming signals can be completely removed while the useful signals are retained after the first-step processing. To achieve this goal, we compute the null space of $\mathbf{Z}_k$ and let $\mathbf{W}_{ak}^H$ be a matrix supported by the null space. The null space can be obtained by computing the singular value decomposition (SVD) of the jamming channel matrix $\mathbf{Z}_k$. Let the left singular vector matrix of $\mathbf{Z}_k$ be $\mathbf{U_z}$. The null space $\mathbf{Q}_k \in \mathbb{C}^{N_k \times (N_k - JN_J)}$ is then obtained from the $(N_k - JN_J)$ columns of $\mathbf{U_z}$ corresponding to the $(N_k - JN_J)$ least singular values (having zero values in the ideal case) . We can then obtain $\mathbf{W}_{ak}$ from $\mathbf{Q}_k$ and $\mathbf{H_k}$, as will be detailed in Section III-B. The determination of $\mathbf{W}_{bk}$ will be described in Section III-C.

Since $\mathbf{W}_{ak}$ is from the null space of $\mathbf{Z}_k$, we have $\mathbf{W}_{ak}^H \mathbf{Z}_k = 0$. Consequently, the jamming signals, $\mathbf{W}_{ak}^H \sum_{j=1}^J \mathbf{Z}_{k,j} \mathbf{f}_j$, are filtered out. The processed signal becomes

$$\mathbf{r_k} = \mathbf{W_{ak}^H H_k} \sum_{i=1}^{K} \mathbf{P_i x_i} + \mathbf{W_{ak}^H n}. \qquad (5)$$

From (5), the combined signal for all users can be expressed as

$$\begin{aligned}
\mathbf{r} &= [\mathbf{r}_1, ..., \mathbf{r}_K]^T \\
&= \begin{bmatrix} \mathbf{W}_{a1}^H \mathbf{H}_1 \\ ... \\ \mathbf{W}_{aK}^H \mathbf{H}_K \end{bmatrix} \mathbf{Px} + \begin{bmatrix} \mathbf{W}_{a1}^H \\ ... \\ \mathbf{W}_{aK}^H \end{bmatrix} \mathbf{n} \\
&= \widetilde{\mathbf{H}} \mathbf{Px} + \mathbf{W}_a^H \mathbf{n}, \qquad (6)
\end{aligned}$$

where $\widetilde{\mathbf{H}} = [\widetilde{\mathbf{H}}_1^T, ..., \widetilde{\mathbf{H}}_K^T]^T$ is an equivalent channel matrix, with $\widetilde{\mathbf{H}}_k = \mathbf{W}_{ak}^H \mathbf{H}_k$, and $\mathbf{W}_a^H = [\mathbf{W}_{a1}^H, ... \mathbf{W}_{aK}^H]^H$. We now have a conventional SDMA system with S_k digital outputs at UE k. Detailed design of $\mathbf{P}$, as well as $\mathbf{W_{bk}}$, is provided in Section III-C.

Depending on how $\mathbf{W}_{ak}$ is designed, UE k may feed back either the equivalent channel $\widetilde{\mathbf{H}}_k$ or $\mathbf{Q}_k^H \mathbf{H}_k$ to the BS.

B. Design of $\mathbf{W}_{ak}$

There are great flexibilities in designing $\mathbf{W}_{ak}$ from $\mathbf{Q}_k$. In this work, we propose two methods. The first one is based on the eigen-beamforming concept. It only requires UE k to know its own channel, and then feedback $\widetilde{\mathbf{H}}_k$ to the BS. The second one is based on the optimization of a sum-rate objective function. It requires the feedback of $\mathbf{Q}_k^H \mathbf{H}_k$ from UE k to the BS, and the BS needs to notify UE k the designed $\mathbf{W_{ak}}$. The second method enables centralized optimization, and can potentially achieve better performance. However, the feedback overhead is larger. In either case, we can represent $\mathbf{W_{ak}}$ as

$$\mathbf{W_{ak}} = \mathbf{Q_k B_k}, \qquad (7)$$

where $\mathbf{B}_k$ is a $(N_k - JN_J) \times S_k$ matrix.

There is an alternative option of using a $\mathbf{B_k}$ with more columns. This results in a system with more flexibility in designing the precoder $\mathbf{P}$, as well as $\mathbf{W}_{bk}$. However, this will increase the required feedback information for the eigen-beamforming design. It does not necessarily lead to improved performance either, as we will show in the simulation results

in Section IV. Our scheme below is presented by referring to the use of minimum number of rows S_k for $\mathbf{B_k}$ here, but it can be extended straightforwardly to other values by replacing S_k with a larger value in the following algorithms.

1) Eigen-beamforming Determined at UE: In this method, multi-user interference is not considered when deciding $\mathbf{B}_k$ at UE k. In this case, $\mathbf{B}_k$ can be determined by selecting S_k eigenvectors corresponding to S_k maximal eigenvalues in the SVD of $(\mathbf{Q}_k^H \mathbf{H}_k \mathbf{H}_k^H \mathbf{Q}_k)$. We denote this method as "Eigen-BF". Designing the Eigen-BF at UE side then feedback to BS is quite different to most of the work in the literature, which generally designs the precoder first directly using the channels. Our method here can lead to less feedback requirement when channel reciprocity is not available, and it also achieves better performance using the precoder designed in this paper.

2) Sum-rate Maximization at BS: In this section, we discuss how to obtain an optimal $\mathbf{W}_{ak}$ from $\mathbf{Q}_k$ to maximize the upper bound of the MU-MIMO sum-rate by referring to the successive interference cancellation (SIC) method in Section IV-B in [13].

Specifically with $\mathbf{W}_{ak} = \mathbf{Q}_k \mathbf{B}_k$, the upper bound of the MU-MIMO sum-rate for our system with equivalent channel matrix $\widetilde{\mathbf{H}}$ can be expressed as

$$\begin{aligned}
R &= \log_2 \left| \mathbf{I} + \frac{P_T}{N_T \sigma^2} \sum_{k=1}^{K} ((\mathbf{Q}_k \mathbf{B}_k)^H \mathbf{H}_k)^H ((\mathbf{Q}_k \mathbf{B}_k) \mathbf{H}_k) \right| \\
&= \sum_{k=1}^{K} \log_2 \left| 1 + \frac{P_T}{N_T \sigma^2} (\mathbf{B}_k^H \mathbf{Q}_k^H \mathbf{H}_k \mathbf{G}_{k-1}^{-1} \mathbf{H}_k^H \mathbf{Q}_k \mathbf{B}_k) \right|,
\end{aligned}$$
$$(8)$$

where

$$\begin{aligned}
\mathbf{G}_k &= \mathbf{I} + \frac{P_T}{N_T \sigma^2} \sum_{i=1}^{k} (\mathbf{B}_i^H \mathbf{Q}_i^H \mathbf{H}_i)^H (\mathbf{B}_i^H \mathbf{Q}_i^H \mathbf{H}_i), \\
\mathbf{G}_0 &= \mathbf{I}, \qquad (9)
\end{aligned}$$

and P_T is the total transmission power.

By applying the SIC principle in [13], we can obtain the optimal matrix $\mathbf{B}_k$ which contains S_k eigenvectors corresponding to S_k maximal eigenvalues in the SVD of $(\mathbf{Q}_k^H \mathbf{H}_k \mathbf{G}_{k-1}^{-1} \mathbf{H}_k^H \mathbf{Q}_k)$. We denote this method as "SIC, Anti-jamming". Since this process requires the knowledge of all UEs' equivalent channels, it is most efficiently implemented in BS.

C. Design Precoding Matrix $\mathbf{P} \in \mathbb{C}^{N_T \times S}$

With $\mathbf{W}_{ak}$ determined, (6) becomes a conventional SDMA system. Here, we design three types of precoders, i.e., zero-forcing (ZF), and improved block diagonalization (IBD), as well as the associated $\mathbf{W}_{bk}$ combiner at UE K. The total transmission power is constrained, so Trace$(\mathbf{P^H P}) \leq \mathbf{P_T}$.

1) ZF Precoder: For the ZF precoder design, we can easily obtain it by channel inversion, which is

$$\mathbf{P^{ZF}} = \widetilde{\mathbf{H}}^{-1} \mathbf{\Lambda}, \qquad (10)$$

where $\mathbf{\Lambda}$ is a diagonal matrix accounting for power normalization and power loading (if desired). Power loading means

allocating transmission power to symbols for different users according to their channel conditions using, e.g., water filling algorithms. Such designs can be referred to [14], and are not further investigated in this paper. We only apply $\mathbf{\Lambda}$ to normalize the power of each column in $\mathbf{P}^{\text{ZF}}$ to be P_T/S.

2) Improved Block Diagonalization: For the IBD precoder design, let us first define $\overline{\mathbf{H}}_k = [\widetilde{\mathbf{H}}_1^T, ..., \widetilde{\mathbf{H}}_{k-1}^T, \widetilde{\mathbf{H}}_{k+1}^T, ..., \widetilde{\mathbf{H}}_K^T]^T \in \mathbb{C}^{(S-S_k)\times N_T}$. The SVD operation is applied to $\overline{\mathbf{H}}_k$ to obtain its null space matrix $\mathbf{Q}_{Pk} \in \mathbb{C}^{N_T \times (N_T-S+S_k)}$, which contains the $(N_T - S + S_k)$ right singular vectors corresponding to the $(N_T - S + S_k)$ least (zero) singular values.

For UE k, the precoding matrix $\mathbf{P_k} \in \mathbb{C}^{N_T \times S_k}$ spans the null space and can be represented as

$$\mathbf{P_k} = \mathbf{Q_{Pk}A_{Pk}\Lambda_k}, \tag{11}$$

where $\mathbf{A_{Pk}} \in \mathbb{C}^{(N_T-S+S_k)\times S_k}$ is a linear mapping matrix to be determined, and $\mathbf{\Lambda_k}$ is a diagonal power normalization or loading matrix.

In order to determine $\mathbf{A_{Pk}}$, we define an equivalent channel $\widehat{\mathbf{H}}_k = \mathbf{W}_{ak}^H \mathbf{H}_k \mathbf{Q}_{Pk}$. Further compute the SVD of $\widehat{\mathbf{H}}_k$ as

$$\widehat{\mathbf{H}}_k = \mathbf{U}_{Pk}\mathbf{\Sigma}_{Pk}\mathbf{V}_{Pk}^H. \tag{12}$$

We can then design $\mathbf{A_{Pk}}$ as the eigen-beamforming of $\widehat{\mathbf{H}}_k$, by choosing it as the partial submatrix of $\mathbf{V}_{Pk}$, i.e., $\mathbf{A_{Pk}}$ contains S_k columns of $\mathbf{V}_{Pk}$ corresponding to the S_k largest singular values.

Although it requires another SVD for each UE, the size of the matrix for SVD computation is $S_k \times (N_T - S + S_k)$ and hence the computational complexity is generally low.

Once $\mathbf{P_k}$'s are obtained for all UEs, the precoding matrix $\mathbf{P}$ is then determined. Such an IBD design ensures ISI-free transmission between any two spatial streams. Compared to ZF precoder, it provides more robustness against channel singularity and hence potentially better performance. However, its complexity is much higher.

3) Design of $\mathbf{W_{bk}}$: When the precoder $\mathbf{P}$ is determined, the combiner $\mathbf{W_{bk}}$ for UE k can be designed based on the combined channel given by

$$\breve{\mathbf{H}}_k = \mathbf{W_{ak}H_kP_k}. \tag{13}$$

The simplest ZF equalizer is given by $\mathbf{W_{bf}} = \breve{\mathbf{H}}_k$. Note that in all the design, the equivalent channel matrix $\breve{\mathbf{H}}_k$ will be diagonal when there is no channel estimation error. More advanced equalizers include minimum mean square error (MMSE), maximal likelihood or sphere decoding, which are well-known techniques, so the details are omitted here.

D. Complexity Analysis

The overall scheme involves several SVD operations, which may make the algorithms seemingly computationally intensive. Actually, only two SVDs at the UE side are necessary for typical scenarios when we use the eigen-beamforming for deciding $\mathbf{B_k}$ at UE and use ZF for precoder at BS. According to simulation results presented in Section IV, there is only minor performance degradation compared to other more advanced designs proposed in this paper.

In this case, computing $\mathbf{Q_k}$ to determine the null space of jamming channels and computing eigen-beamforming both need an SVD operation at each UE. When the number of total jamming antennas is small, $\mathbf{Z_k}$ has a limited number of columns and the complexity of SVD operation for obtaining $\mathbf{Q_k}$ is not very high. The number of independent streams for each UE in an MU-MIMO system is generally small. Hence the required SVD operation for getting $\mathbf{B_k}$ can be efficiently computed using, e.g., the power method.

IV. SIMULATION RESULTS

This section presents the simulation results using MATLAB to validate our proposed scheme. The adopted performance metrics include the bit error rate (BER) and the sum-rate. The simulation configurations are as follows, unless otherwise stated.

A tactical MU-MIMO system is simulated. Note that BS and UE here can directly be replaced by nodes in a stationary ad-hoc network. Both BS and each UE are equipped with 8 antennas (e.g., $N = N_T = N_k = 8$), and BS sends 1 spatial stream to each of 4 users. We consider a jamming scenario with $J = 2$ single-antenna jammers distributed at different locations. The ratio of jamming power to signal of interest power is 1, which cause received SINR lower than 0 dB. We apply 16 Quadrature Amplitude Modulation (QAM) with no forward error correction (FEC) coding. We simulate a narrowband system with single carrier modulation.

The total number of multipath between BS and each UE is 5. The AoAs of multipath for the user and jammer are uniformly distributed in the range of $[\theta_{a,k} - \alpha_a, \theta_{a,k} + \alpha_a]$ and $[\phi_{a,j} - \alpha_a, \phi_{a,j} + \alpha_a]$, where $\theta_{a,k} = 120$ and $\phi_{a,j} = 150$ degrees are the AoAs of the LOS path for user k and jammer j, respectively, and the angle spread α_a is 80 degrees. The AoDs of multipath for the user and jammer are uniformly distributed in the range of $[\theta_{d,k} - \alpha_d, \theta_{d,k} + \alpha_d]$ and $[\phi_{d,j} - \alpha_d, \phi_{d,j} + \alpha_d]$, where $\theta_{d,k} = \phi_{d,j} = 80$ degrees are AoDs of the LOS path for user k and jammer j, respectively, and the angle spread α_d is 360 degrees. The power ratio between the LOS and non-LOS (NLOS) path, which is known as the Rician factor, is set to 5 and 10 for UEs and jammers, respectively.

We use captions "Rx Eigen-BF" and "Rx SIC, anti-jamming" for the cases when the two combiners presented in Section III-B are used, respectively. Since we have not been able to find existing work on the same topic with our paper, we provide comparison with a benchmark algorithm based on the sum-rate maximization without considering the existence of jamming signals. In other words, when deriving the combiner $\mathbf{W_{ak}}$ using (8), we remove the matrix $\mathbf{Q_k}$ from the equation. We then test the obtained $\mathbf{W_{ak}}$, together with the precoders proposed in this paper, for cases when the jamming signal is present or absent. We denote the two cases as "SIC, No Anti-Jam" and "SIC, No Jam", respectively.

In Fig. 2, we show the BER performance of our proposed schemes. The figure shows that in the presence of jamming signals, conventional receiver such as "SIC, No Anti-Jam" fails to work. Our proposed anti-jamming algorithms can effectively suppress jamming while supporting MU-MIMO. IBD shows
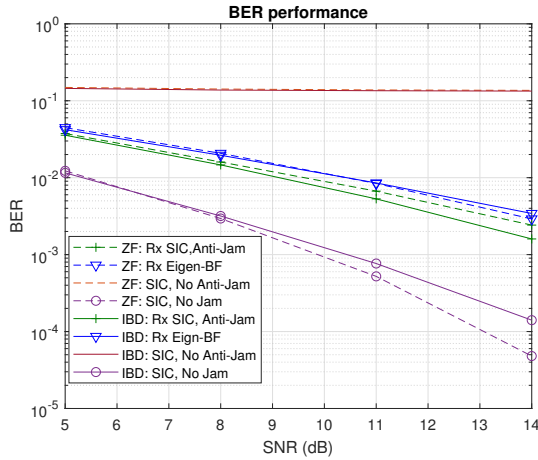
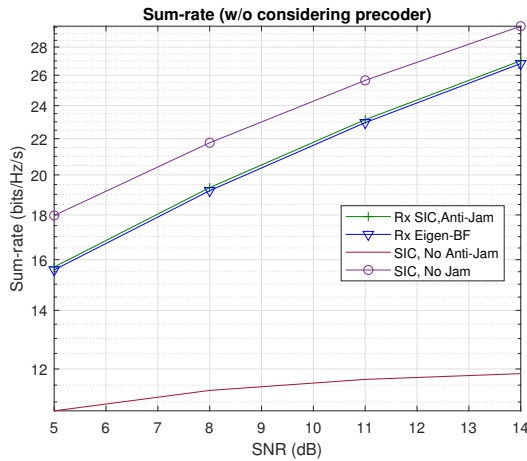Fig. 2. BER versus SNR for different combiners and precoders, where BS sends one stream to each of four UEs.

Fig. 4. BER versus the number of UEs, where SNR=10 dB and the IBD precoder is used.

Fig. 3. Sum-rate versus SNR for different combiners and precoders, where BS sends one stream to each of four UEs.

Fig. 5. BER (left) and sum-rates (right) for two different antenna configurations: Setup 1 (solid curves): BS sends 1 stream to each of 8 UEs, and each UE has 4 antennas; and Setup 2 (dashed curves): BS sends 2 streams to each of 4 UEs, and each UE has 8 antennas. BS has 16 antennas, ZF precoder is used, and Rician factor is 1.

slightly better performance than ZF precoder. The performance loss due to combating jamming is also significant, and is approximately 5 dB at BER=10^{-3}, referring to the "SIC, No Jam" curve.

Fig. 3 demonstrates the sum-rates of various algorithms. The sum-rate is computed based on (8). It takes into consideration the jamming signal power but does not include the precoder **P**. The sum-rates represent the upper bound capacity that the MU-MIMO system can achieve. Except for "SIC, No Jam" which does not consider jamming signals, the other three have jamming in place. There is a loss of approximately 2 bits/Hz/s due to jamming suppression. The improvement of the proposed schemes with respect to the case no jamming suppression is significant. The sum-rate results are consistent with the BER results in Fig. 2.

In Fig. 4, we demonstrate how the BER performance varies with the number of UEs when BS sends one stream to each UE. As can be seen, more UEs lead to higher BER for all algorithms. This is because channels become more correlated when more UEs need to be supported using SDMA in the limited spatial domain in the simulation.

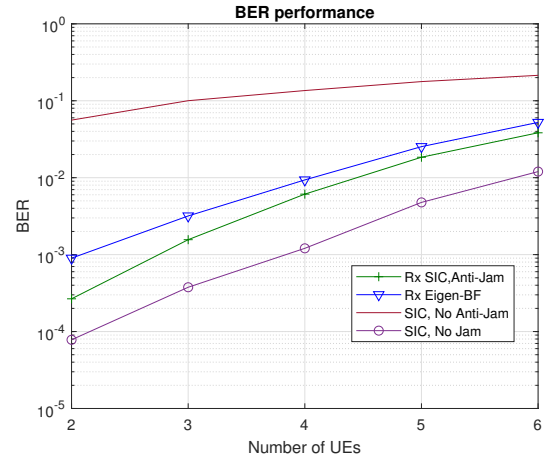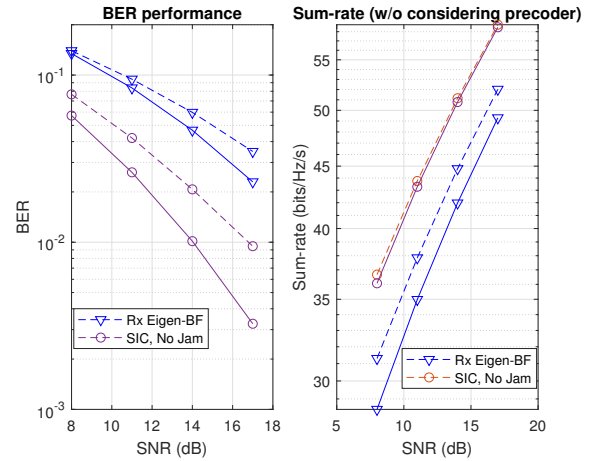In Fig. 5, we present both BER and sum-rates for two cases

when the total number of UE antennas is fixed, but spatial streams and number of antennas per UE are changed. The figure indicates that the sum-rates for the two cases are similar for the proposed scheme when only the combiner $\mathbf{W_{ak}}$ at UEs are taken into consideration in the equivalent channels. With the specifically used ZF precoder, the case with fewer streams per UE has lower BER due to lower channel correlation and therefore lower noise enhancement effect. For both cases, the proposed scheme works well, but with degraded performance compared to the cases with $N_T = 8$ and $S = 4$. This is because an increased number of streams leads to increased channel correlation.

In Fig. 6, we show how BER is affected when we use a $\mathbf{B_k}$ with different number of columns. The figure shows that with the number of columns increasing, the BER increases. Although a strict proof is not available at this stage, intuitively this can be explained as follows. With $\mathbf{Q_k}$ decided, the equivalent channel $\mathbf{Q_k^H H_k}$ is given. Hence without considering precoder, the optimal combiner for achieving S_k streams is given by the eigenbeam matrix corresponding to the S_k
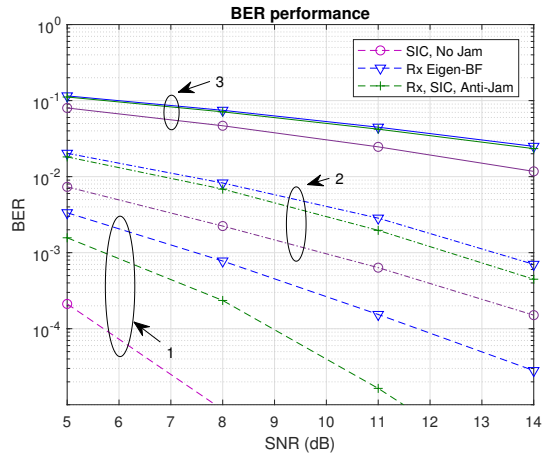
Fig. 6. Variation of BER with the number of columns in $\mathbf{B}_k$: 1 (dashed curves), 2 (dashed-dotted curves) and 3 (solid curves), where the Rician factor is 3, the number of antennas at BS and each UE is 16, and IBD precoder is used.
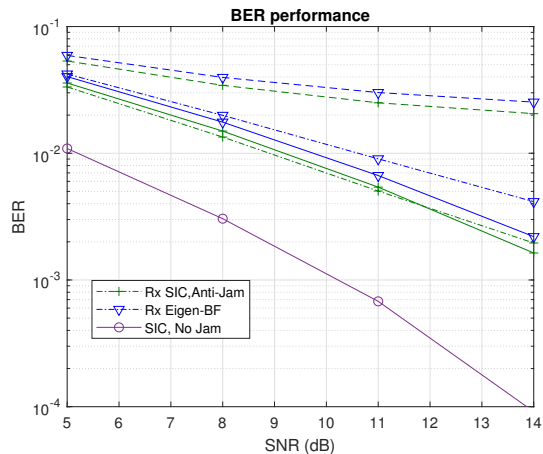

Fig. 7. Variation of BER with the estimation error of jamming channels. The variance of approximation error σ_h^2 is 0.1 (dashed curves), 0.01 (dashed-dotted curves) and 0.0001 (solid curves). ZF precoder is used.

maximal eigenvalues of $\mathbf{Q}_\mathbf{k}^\mathbf{H}\mathbf{H}_\mathbf{k}\mathbf{H}_\mathbf{k}^\mathbf{H}\mathbf{Q}_\mathbf{k}$. At the same time, more columns of $\mathbf{Q}_\mathbf{k}$ leads to potentially larger multi-user interference and smaller null space of $\bar{\mathbf{H}}_k$ and hence fewer columns in $\mathbf{Q}_{\mathbf{Pk}}$. This causes overall performance degradation.

Finally, we assess the performance of the proposed scheme in the presence of channel estimation errors for the jamming channel. Such errors could always be present in practical systems due to the non-cooperative nature of jamming sources. The errors are approximately AWGN with zero mean and variance σ_h^2, in relation to the jamming channels when its mean power is 1. Fig. 7 demonstrates how BER varies with the channel estimation error represented via σ_h^2. The figure shows that the proposed scheme still performs well when $\sigma_h^2 = 0.01$, though performance degradation is significant when $\sigma_h^2 = 0.1$.

V. CONCLUSION

We proposed a scheme for supporting MU-MIMO downlink communications in the presence of high-power jammers. Setting jamming suppression as the highest priority, we first constructed a combiner at UE receiver to fully remove jamming signals, assuming that the jamming channels are perfectly known. Such a combiner spans over the null space of the jamming channels. We then proposed two methods for determining a linear mapping matrix based on the null space. Based on the equivalent channel each UE feeds back, we further proposed two algorithms, zero forcing and improved block diagonalization, to design the BS precoder. Extensive simulation results are presented and demonstrate that the proposed scheme is able to effectively suppress jamming signals while supporting MU-MIMO communications.

REFERENCES

[1] Q. H. Spencer, A. L. Swindlehurst, and M. Haardt, "Zero-forcing methods for downlink spatial multiplexing in multiuser MIMO channels," *IEEE Transactions on Signal Processing*, vol. 52, no. 2, pp. 461–471, Feb 2004.

[2] A. Knopp, R. T. Schwarz, and B. Lankl, "MIMO system implementation with displaced ground antennas for broadband military SATCOM," in *2011 - MILCOM 2011 Military Communications Conference*, Nov 2011, pp. 2069–2075.

[3] H. Luo, D. Xu, and J. Bao, "Outage capacity analysis of MIMO system with survival probability," *IEEE Communications Letters*, vol. 22, no. 6, pp. 1132–1135, June 2018.

[4] J. R. Pennington and R. K. Martin, "Utilization of inter-block interference in MIMO-OFDM communication systems," in *MILCOM 2018 - 2018 IEEE Military Communications Conference (MILCOM)*, Oct 2018, pp. 163–168.

[5] S. Zhang, K. Huang, and X. Li, "Adaptive transmit and receive beamforming based on subspace projection for anti-jamming," in *2014 IEEE Military Communications Conference*, Oct 2014, pp. 388–393.

[6] J. L. J.-W. C. Sung-Ho Lim, Sungmin Han, "Tactical beamforming against high-power reactive jammer," in *2016 Eighth International Conference on Ubiquitous and Future Networks (ICUFN)*, July 2016, pp. 92–95.

[7] V. Ramaswamy, J. R. Fevold, J. T. Correia, and T. E. Daughters, "Design of an anti-jamming appliqué for LTE-based military communications," in *MILCOM 2016 - 2016 IEEE Military Communications Conference*, Nov 2016, pp. 230–235.

[8] A. Kekirigoda and K. Hui, "Tactical line-of-sight MIMO communication system for contested networks," in *2017 27th International Telecommunication Networks and Applications Conference (ITNAC)*, Nov 2017, pp. 1–6.

[9] W. Rui, "Research and implementation of anti-jamming methods for military communication," in *2018 11th International Conference on Intelligent Computation Technology and Automation (ICICTA)*, Sep. 2018, pp. 167–171.

[10] N. Zhao, J. Guo, F. R. Yu, M. Li, and V. C. M. Leung, "Antijamming schemes for interference-alignment-based wireless networks," *IEEE Transactions on Vehicular Technology*, vol. 66, no. 2, pp. 1271–1283, Feb 2017.

[11] T. T. Do, E. Björnson, E. G. Larsson, and S. M. Razavizadeh, "Jamming-resistant receivers for the massive MIMO uplink," *IEEE Transactions on Information Forensics and Security*, vol. 13, no. 1, pp. 210–223, Jan 2018.

[12] X. Wei, Q. Wang, T. Wang, and J. Fan, "Jammer localization in multi-hop wireless network: A comprehensive survey," *IEEE Communications Surveys Tutorials*, vol. 19, no. 2, pp. 765–799, Secondquarter 2017.

[13] J. A. Zhang, H. Li, X. Huang, Y. J. Guo, and A. Cantoni, "User-directed analog beamforming for multiuser millimeter-wave hybrid array systems," in *2017 IEEE 85th Vehicular Technology Conference (VTC Spring)*, June 2017, pp. 1–5.

[14] V. Stankovic and M. Haardt, "Generalized design of multi-user mimo precoding matrices," *IEEE Transactions on Wireless Communications*, vol. 7, no. 3, pp. 953–961, March 2008.